

# MAGNETIC-FIELD CALCULATIONS FOR THE MAGNETS OF THE HIGH-ENERGY STORAGE RING (HESR) AT FAIR\*

H.Soltner<sup>#</sup>, U.Bechstedt, R.Tölle, Forschungszentrum Jülich GmbH (FZJ), Jülich, Germany  
J.G. de Villiers, iThemba Labs, Somerset West, South Africa

## Abstract

FZJ is responsible for the design and construction of the HESR [1], as a contribution to the future Facility for Antiproton and Ion Research (FAIR) [2] at GSI in Darmstadt, Germany. This task comprises the layout and provision of the dipole, quadrupole, and sextupole magnets and the floor management. All the magnets will be iron-dominated and normal-conducting. Magnetic-field calculations have been carried out in order to optimize the pole shapes of the magnets and their end chamfers, with the goal to reduce the higher harmonics for each magnet. This publication reports on the results of these calculations.

## OVERVIEW OF THE HESR

Figure 1 shows the overall layout of the HESR. The design of the lattice is the result of detailed beam dynamics calculations. The general layout has already been described in an earlier publication [1].

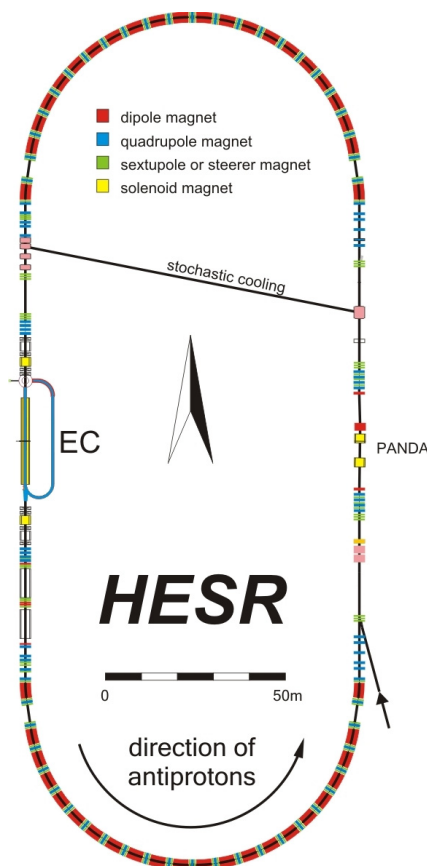


Figure 1: Design of the future HESR for FAIR.

\* Work supported by BMBF and NRF, Project code SUA 06 / 003  
<sup>#</sup> h.soltner@fz-juelich.de

## MAGNET LAYOUT

### Overview of Magnets

The HESR lattice will comprise 44 dipole magnets, 84 quadrupole magnets, and 60 sextupole magnets. Table 1 gives an overview of their characteristics, and Figure 2 shows their design.

The dipole magnets have a finite radius of curvature in order to keep the circulating particles closer to the centre of the magnets, where the field is more homogeneous. On the other hand, this curvature introduces additional higher harmonics, as has already been investigated for previous magnet designs [3].

Table 1: Properties of the Magnets

	dipole	quadrup.	sextupole
aperture	100 mm	100 mm	140 mm
eff. length	4,200 mm	600 mm	300 mm
curvature	29.432 m	-	-
<u>Yoke</u>			
length	4.126 m	0.58 m	0.3 m
width	1.142 m	1.06 m	0.45 m
height	0.62 m	1.06 m	0.45 m
mass	19.27 t	4.3 t	0.160 t
<u>Coils</u>			
numb. coils	2	4	6
turns / coil	24	50	15
layers / coil		4	2
wind. / layer	6	14,13,12,11	7.5
conductor	35 x 20 mm <sup>2</sup>	15 x 8 mm <sup>2</sup>	10.6 x 7 mm <sup>2</sup>
cooling bore	12 mm	4.5 mm	4 mm
current dens.	5.02 A/mm <sup>2</sup>	4.13 A/mm <sup>2</sup>	4.77 A/mm <sup>2</sup>
voltage	43.8 V	28.12 V	1.92 V
power	64.17 kW	3.0 kW	0.296 kW
<u>Magnet data</u>			
mass	24,000 kg	5,200 kg	220 kg
inductance	37 mH	46.4 mH	3.4 mH
power	128.34 kW	12.0 kW	1.8 kW
water flow	61.6 l/min	6.4 l/min	0.86 l/min

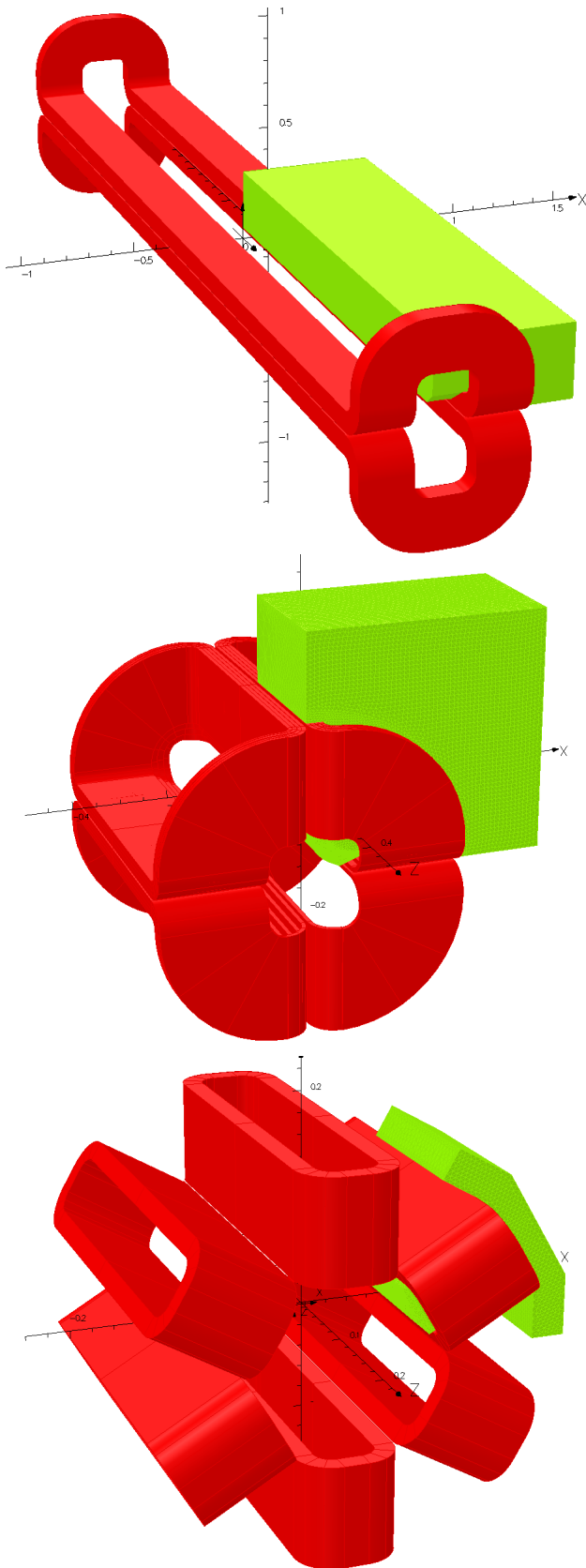


Figure 2: Overview of the coil geometry (shown in red) and part of the yoke (in green) for the three magnet types. Only an eighth (dipole and quadrupole) or a twelfth (sextupole) of the iron yoke is shown for visual clarity.

### Multipole Calculations

As a first step, the cross sections of the magnets were optimized with the 2D software package MAGNETO [4], such that the variation of the absolute value of the B field along the reference circle (33 mm radius for dipole and quadrupole, 44 mm radius for the sextupole) showed minimum variation. The optimized cross sections were rebuilt in the software package TOSCA [5] and extruded in the 3<sup>rd</sup> dimension, based on the design length of the magnet. The Fourier transforms of the radial flux density distributions on reference circles at representative locations along the beam axis were analyzed using self-written programs in MathCad or Excel. To comply with conventions, the multipole components were normalized by assigning a value of  $10^4$  to the main field component. In an iterative process appropriate chamfers at the ends of the magnet poles were introduced to reduce the integrals of the higher harmonics taken along the beam direction.

### Results for Dipoles, Quadrupoles and Sextupoles

The design of the H-type dipole is shown in the upper part of Figure 2. Two types of 3D simulations have been carried out. The first one disregards the curvature of the magnet in order to be able to assign a realistic packing factor of 95% to the yoke iron. The second one takes the curvature into account, but inevitably has to assign a packing factor of 100%, as a combination of these two features is not available. Table 2 shows the results of these calculations. The dipoles are to be operated between excitations with flux densities from 0.17 T to 1.7 T, at a reference point, taken on the median plane at the centre of the gap. On request the yoke geometry was optimized for 1.0 T, and consequently larger harmonic disturbances for other excitations will appear. Particle injection is done at 0.43 T.

Table 2: Integrated multipole components and effective lengths for the dipole at various excitation currents.

dipole	curved	curved	curved	straight
Flux dens.	0.17 T	1.0 T	1.7 T	1.0 T
2 pole	10 000	10 000	10 000	10 000
4 pole	-0.03	0.01	0.10	
6 pole	-4.32	0.72	28.16	-1.98
8 pole	0.04	0.06	0.09	
10 pole	-1.62	-0.05	6.03	-0.33
12 pole	0.01	0.01	0.01	
14 pole	-0.06	0.10	0.43	-0.16
16 pole	0.00	0.00	0.00	
18 pole	0.00	0.04	0.00	-0.05
20 pole	0.06	0.00	-0.10	
Eff. length	4.229 m	4.228 m	4.220 m	4.228 m

Due to the curvature of the dipole small values of higher harmonics appear, that are not present in straight dipoles for symmetry reasons. The black curve in Figure 3 shows the variation of the sextupole component in the case of the straight dipole as its largest error harmonic.

Table 3 gives the results of the corresponding calculations for the quadrupole and the sextupole that are shown in the middle and lower part of Figure 2. With all three types of magnets the calculated triple-multipoles are respectively the main contributors to the higher order magnetic disturbances. The variation of these main contributors at the respective exit edges of the magnets are shown in Figure 3. Although the variations are relatively large, the integrated values nearly cancel, because the area between the two lobes in each of the bipolar curves have been made almost the same by choosing a  $50^\circ$  chamfer angle for each of the magnet types.

Table 3: Integrated multipole components and effective lengths for the quadrupole and sextupole magnets.

	Quadrupole	Sextupole
4 pole	10 000	
6 pole		10 000
8 pole	-0.08	
10 pole		0.00
12 pole	-0.20	
14 pole		0.00
16 pole	0.00	
18 pole		-0.70
20 pole	-0.17	
Eff. length	0.61 m	0.33 m

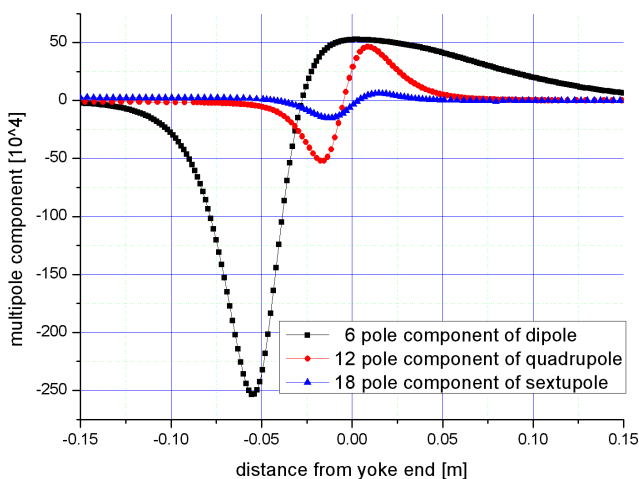


Figure 3: Triple-harmonics contributions to the magnetic fields towards the ends of the individual magnets.

## CONCLUSIONS

For this work the principal magnets for the HESR have been optimized. The curvature of the dipole magnets introduces only very small changes to the multipole values as compared to a straight magnet. For all the magnets the first allowed higher harmonics were found to be the most pronounced ones. It could be shown that in most cases they can be kept within an acceptable range for all the specified excitations. This goal was achieved by introducing chamfers of  $50^\circ$  at the ends of the magnet yokes. The only concern at present is the high sextupole component of the dipole magnets of about 28 units at an excitation of 1.7 T, see Table 2. Because the sextupole magnets are not designed to compensate more than 10 units, the sextupole component of the dipole must be limited to this value. The sextupole component at high excitations can be reduced by the introduction of air gaps inside the yoke, which divert the magnetic flux towards the outer region at the expense of a somewhat higher power consumption of the magnets.

In practice, however, the magnets will be located very close to each other due to space restrictions, which lead to the interference of the magnetic fields of neighbouring magnets. In particular, the sextupoles for compensation of the sextupole component of the dipoles are located within the strong stray field of the dipoles. This results in a reduction of the effective length of the dipoles and the generation of other harmonics. Therefore, the optimization of isolated magnets without interference from neighbouring ones, as it was performed for this study, can only be the first step in order to realistically assess the performance of the entire magnet assembly in this case. Results on these interference effects will be the subject of a future publication.

## REFERENCES

- [1] R.Toelle *et al.*, "HESR at Fair: Status of Technical Planning", PAC07, Albuquerque, NM, USA, TUPAN024, p. 1442 (2007); <http://www.JACoW.org>
- [2] FAIR Baseline Techn. Report, Darmstadt 2006, vol. 2, p. 511 ff; [http://www.gsi.de/fair/reports/btr\\_e.html](http://www.gsi.de/fair/reports/btr_e.html)
- [3] H.Soltner, U.Pabst, and R.Toelle, "Magnetic Field Calculations of the Superconducting Dipole Magnets for the High-Energy Storage Ring at FAIR", PAC07, Albuquerque, NM, USA, MOPAN021, p. 194 (2007); <http://www.JACoW.org>.
- [4] MAGNETO by Integrated Engineering Software, Winnipeg, CAN.; <http://www.ies.com>.
- [5] TOSCA by Cobham Technical Services, Kidlington, UK; <http://www.cobham.com/technicalservices>.